

SCIENTIFIC REPORTS

OPEN

Hexacoordinated nitrogen(V) stabilized by high pressure

Dominik Kurzydłowski^{1,2} & Patryk Zaleski-Ejgierd³

Received: 14 June 2016
Accepted: 10 October 2016
Published: 03 November 2016

In all of its known connections nitrogen retains a valence shell electron count of eight therefore satisfying the golden rule of chemistry - the octet rule. Despite the diversity of nitrogen chemistry (with oxidation states ranging from +5 to -3), and despite numerous efforts, compounds containing nitrogen with a higher electron count (hypervalent nitrogen) remain elusive and are yet to be synthesized. One possible route leading to nitrogen's hypervalency is the formation of a chemical moiety containing pentavalent nitrogen atoms coordinated by more than four substituents. Here, we present theoretical evidence that a salt containing hexacoordinated nitrogen(V), in the form of an NF_6^- anion, could be synthesized at a modest pressure of 40 GPa (=400 kbar) via spontaneous oxidation of NF_3 by F_2 . Our results indicate that the synthesis of a new class of compounds containing hypervalent nitrogen is within reach of current high-pressure experimental techniques.

Since the first synthesis of the NF_4^+ cation in 1966¹ numerous experimental attempts have been made to synthesize its neutral parent molecule, NF_5 ²⁻⁵. All of these attempts turned out fruitless, eventually leading to the conclusion that the highest coordination number (CN) attainable for pentavalent nitrogen is 4, with higher CNs not possible due to steric hindrance around the nitrogen atom⁶. Obviously, it's possible to find nitrogen in an environment with higher CNs, but only in salts containing the isolated, and non-hypervalent, N^{3-} anion (e.g. Li_3N exhibiting 8-fold N coordination)⁷, or in certain coordination complexes of trivalent nitrogen (e.g. $[(\text{Ph}_3\text{PAu})_5\text{N}]^{2+}$)⁸ in which, despite the high CNs, the valence shell electron count on nitrogen never exceeds eight.

Theoretical investigations into the properties of the nitrogen pentafluoride molecule (NF_5) in the gas phase⁹⁻¹³ indicate that although it is a minimum on the potential energy surface (PES)¹¹⁻¹³, its decomposition into NF_3 and F_2 is highly exothermic (+1.82 eV per NF_5)^{12,13}. Regarding the geometry of the molecule, the ground state structure of NF_5 is a trigonal bipyramid with five covalent N-F bonds. Interestingly the energy of formation of the molecule is comparable with that of solid $(\text{NF}_4^+)(\text{F}^-)$ ¹⁴, making the NF_5 system an interesting example of the interplay between covalent and ionic bonding.

In this communication we present results of a comprehensive computational investigation on the possibility of synthesizing solid NF_5 from NF_3 and F_2 through the application of external pressure in the range of several dozens GPa (1 GPa = 10 kbar). At present pressures up to 200 GPa are routinely achieved in diamond anvil cells (DACs), and the large influence of such high-pressure (HP) conditions on the properties and reactivity of the elements and chemical compounds is well documented¹⁵⁻¹⁸. The potential of obtaining novel species through the application of HP is exemplified inter alia by the recent synthesis of nitrogen analogues of alkanes¹⁹, or by the theoretical predictions that hypervalent carbon species can be stabilized at large compression²⁰.

Most importantly the oxidative strength of fluorine has been predicted to increase considerably at elevated pressures with calculations indicating that at such conditions F_2 should oxidize Cs to CsF_3 ^{21,22}, HgF_2 to HgF_3 ²³, and Ar to ArF_2 ²⁴. Furthermore both theoretical²⁵⁻²⁸ and experimental^{19,29-31} high-pressure studies on the N/H system (analogous to the N/F system studied here) indicate that a wealth of exotic N_xH_y structures should, and indeed does stabilize at HP conditions.

Results

Computational approach. Our solid-state calculations, performed within the Density Functional Theory, in the 0–300 GPa pressure range, utilized the hybrid HSE06 functional³²⁻³⁴. Importantly, benchmark calculations conducted for isolated molecules, indicate that this functional reproduces much better the gas-phase thermodynamic stability of nitrogen fluorides compared to the PBE functional³⁵ typically used “by default” in HP solid-state calculations (for more details see sections I and II of the Supplementary Information, SI). Candidate

¹Centre of New Technologies, University of Warsaw, Warsaw 02-097, Poland. ²Faculty of Mathematics and Natural Sciences, Cardinal Stefan Wyszyński University in Warsaw, Warsaw 01-938, Poland. ³Institute of Physical Chemistry, Polish Academy of Sciences, Warsaw 01-224, Poland. Correspondence and requests for materials should be addressed to D.K. (email: d.kurzydowski@cent.uw.edu.pl) or P.Z.-E. (email: pze.work@gmail.com)

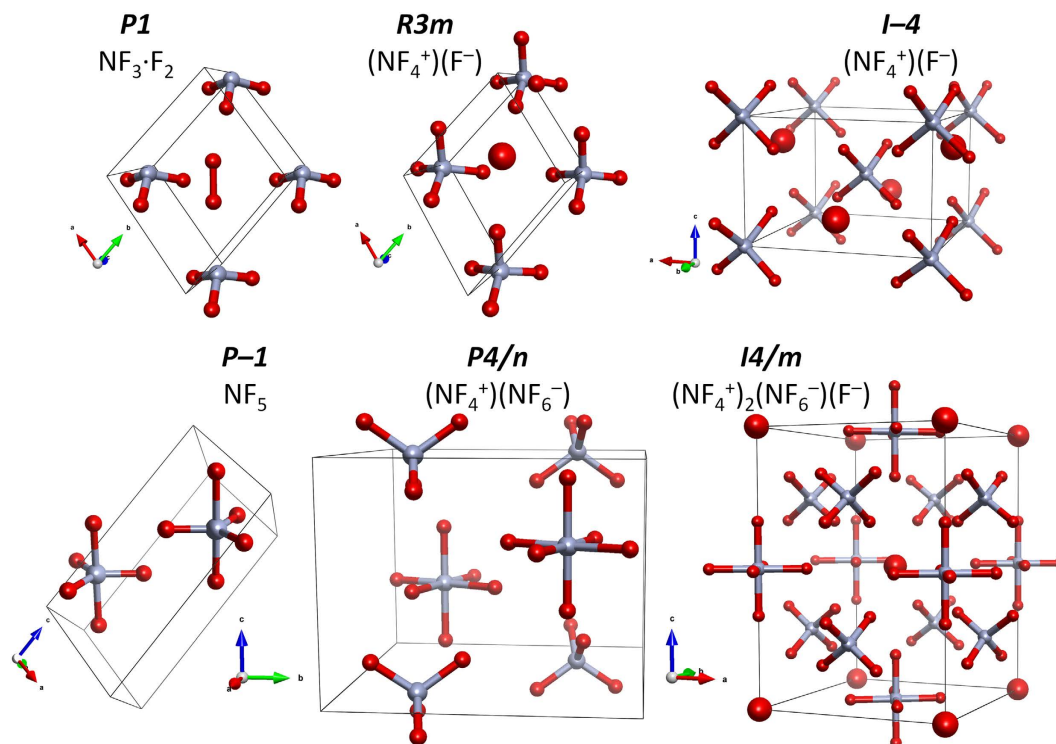


Figure 1. Structures of solid NF_5 . Nitrogen/fluorine atoms are marked by blue/red spheres (covalently bound F atoms are marked with smaller spheres while the F^- anions with larger ones).

structures of NF_5 were identified through the application of the USPEX evolutionary algorithm^{36,37}. The search for the enthalpically best structures revealed a surprising diversity of high-pressure NF_5 polymorphs exhibiting numerous and versatile bonding patterns. All thermodynamic and structural parameters reported here are obtained with the use of the HSE06 functional.

Structures of NF_5 . The lowest enthalpy structures of NF_5 are shown in Fig. 1; for the purpose of this communication we label them with their respective space group symbols. The *P1* structure is a molecular crystal consisting of NF_3 and F_2 molecules, and is the only polymorph containing trivalent nitrogen. Similarly, the *P-1* structure is also a molecular crystal, but in contrast it is composed of *isolated* NF_5 units. Both *R3m* and *I-4* structures exhibit ionic character and both contain NF_4^+ cations and F^- anions. The *I4/m* and *P4/n* phases are also ionic, but apart from the NF_4^+ and/or F^- ions they both contain the NF_6^- anion in which pentavalent nitrogen is bonded to *six* fluorine atoms. This anion was first proposed by Ewig and Van Wazer¹¹ who found it to be dynamically stable in the gas phase, and indeed thermodynamically more stable than $\text{NF}_5 + \text{F}^-$. To our best knowledge there have been no prior reports on the stabilization of NF_6^- in the solid state.

The assignment of ionic/neutral NF_n^{m+} fragments is based not only on the fact that the optimized geometry of these fragments agrees well with that predicted by the VSEPR model³⁸ (NF_3 – trigonal pyramid, NF_4^+ – tetrahedron, NF_5 – trigonal bipyramid, NF_6^- – octahedron), but also on the excellent accordance between the bond lengths of these moieties at effectively 0 GPa and those obtained from gas-phase calculations (Table 1). It's noteworthy to point that even at 300 GPa the NF_n^{m+} fragments remain well-defined, although in some cases quite distorted (*vide infra*). This is best exemplified by the fact that at 300 GPa the secondary $\text{N}\cdots\text{F}$ contacts of all structures are more than 25% longer than the intramolecular N–F bonds, while $\text{F}\cdots\text{F}$ distances are more than 30% longer compared to the genuine F–F bond in a F_2 molecular crystal optimized at the same pressure. As expected all of the studied NF_5 polymorphs are wide-gap insulators with the band gap exceeding 5 eV even at 300 GPa.

The structures optimized with the PBE functional exhibit similar geometries to those described above (obtained with HSE06). Most importantly, we have compared the PBE and HSE06-optimized structure and found no evidence of a Peierls distortion ensuing after optimization of the PBE structures conducted with HSE06, in contrast to what was found for a polymeric phase of nitrogen³⁹. We attribute it to the fact that the studied structures contain isolated ions or molecules, and do not exhibit extended motifs (chains, layers) for which one can expect a Peierls distortion. Finally, we note that while the resulting geometries remain essentially identical for the two functionals the relative enthalpies of various structures differ quite substantially; as already mentioned, in this report we focus on the HSE06 values (for details on the PBE/HSE06 enthalpy differences see Section II of SI).

Stability and pressure evolution of NF_5 polymorphs. Surprisingly, despite the large diversity of bonding patterns exhibited by the structures containing pentavalent nitrogen their relative enthalpies at low pressure fall in a narrow range of 0.6 eV per NF_5 unit (≈ 58 kJ/mol); see Fig. 2.

Moiety	NF ₅ polymorph	Gas phase ^a	0 GPa
NF ₃	<i>P1</i>	1.36 (x3)	1.37 (x3)
(NF ₄ ⁺)	<i>R3m</i>	1.30 (x4)	1.31 (x4)
	<i>I-4</i>		1.31 (x4)
	<i>P4/n</i>		1.31 (x4)
	<i>I4/m</i>		1.31 (x4)
NF ₅	<i>P-1</i>	ax: 1.58 (x2)	ax: 1.58 (x2)
		eq: 1.36 (x3)	eq: 1.37 (x3)
NF ₆ ⁻	<i>I4/m</i>	1.55 (x6)	ax: 1.53 (x2)
			eq: 1.55 (x4)
	<i>P4/n</i>		ax: 1.50, 1.57
			eq: 1.55 (x4)

Table 1. Comparison of calculated N–F bond lengths (in Å) of NF_n^{m+} moieties in the gas phase and in various NF₅ phases (ax – axial, eq – equatorial bonds). ^aValues obtained by geometry optimization of molecular fragments utilizing the HSE06 functional and the *cc-pVQZ* basis set.

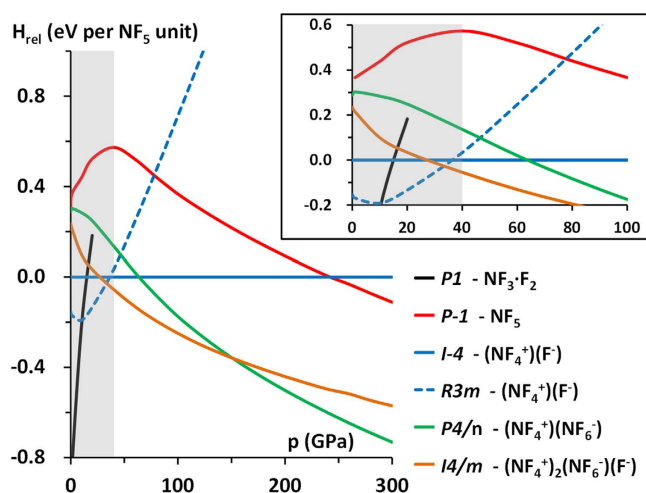


Figure 2. Pressure dependence of the relative enthalpy of NF₅ polymorphs. At each pressure point the enthalpies (obtained with HSE06 calculations) are referenced to that of *I-4*. The grey region marks the pressure range where the enthalpy change of the reaction NF_{3(s)} + F_{2(s)} → NF_{5(s)} is positive ($p < 40$ GPa) indicating instability of NF₅ towards decomposition into NF₃ and F₂.

At pressures lower than 11 GPa it is the *P1* phase ($Z = 1$), containing molecular N^{III}F₃ mixed with F₂, which is the lowest enthalpy structure. Interestingly upon compression of the *P1* structure the F–F bond in F₂ lengthens from 1.39 Å at 0 GPa to 1.44 Å at 39 GPa, while the shortest secondary N⋯F contact contracts from 3.14 Å to 1.89 Å. This points to a significant pressure-induced enhancement of the donor-acceptor interactions between the HOMO of NF₃ and the antibonding LUMO of F₂. In fact, upon compression to 40 GPa this interaction leads to heterolytic dissociation of the F₂ molecules and formation of an ionic structure containing NF₄⁺ cations separated by F⁻ anions. At 40 GPa the shortest F⋯F contact in *P1* is 2.17 Å and the four N–F bonds have a length of 1.29 Å. Those changes clearly illustrate that compression of the *P1* phase up to 40 GPa leads to spontaneous oxidation of N^{III}F₃ by F₂ and subsequent formation of N^VF₄⁺ and F⁻.

Note that at 40 GPa the oxidized *P1* phase turns out to be identical in terms of geometry with another NF₅ polymorph, *R3m* ($Z = 3$, Fig. 1). The coordination of the F⁻ anion in the latter structure is such that each F⁻ is surrounded by 11 F atoms originating from 7 NF₄⁺ cations. In particular, the *R3m* polymorph becomes the ground state structure of the NF₅ system already above 11 GPa. Our USPEX searches identify yet another (NF₄⁺)(F⁻) structure of the *I-4* symmetry ($Z = 2$), which is even more densely packed than the *R3m* (F⁻ anions surrounded by 12 F atoms originating from 8 NF₄⁺ cations). This structure is noteworthy since the *I-4* phase becomes more stable than the *R3m* polymorph at 37 GPa. Nevertheless, already above 33 GPa both *I-4* and *R3m* have a higher enthalpy than a more complex *I4/m* phase ($Z = 6$), which remains the lowest-enthalpy structure up to 151 GPa (see Fig. 2).

The *I4/m* phase is characterized by alternating (NF₆⁻)(F⁻) and (NF₄⁺)₂ layers leading to a general formula of (NF₄⁺)₂(NF₆⁻)(F⁻) = 3NF₅. This structure bears many similarities to the HP phase of PCl₅ (*I2/m* symmetry) which is best formulated as (PCl₄⁺)₂(PCl₆⁻)(Cl⁻)⁴⁰. The *I2/m* polymorph is also layered, but in contrast to the *I4/m* structure of NF₅ it exhibits tilting of the complex ions about an axis lying in the plane of the layers. Geometry

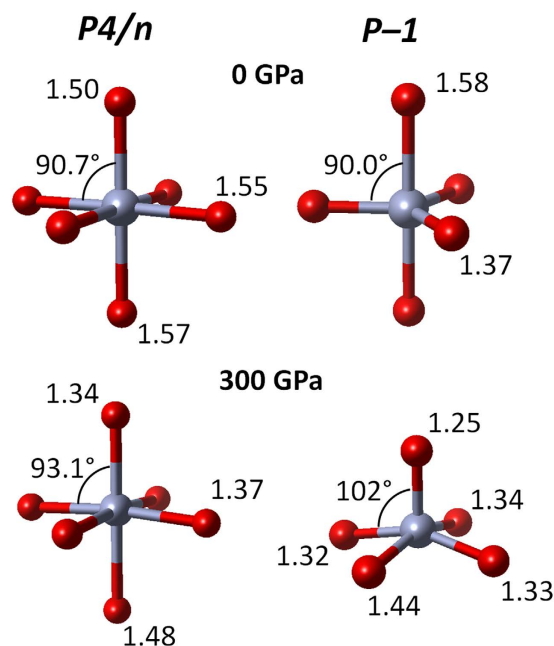


Figure 3. The geometry of the NF_6^- and NF_5 fragments. The NF_6^- fragment in $P4/n$ at 0 and 300 GPa (left) and the NF_5 fragment in $P-1$ at the same pressures (right). Bond distances (in Å) and angles between the axial and equatorial bonds are indicated.

optimization of a NF_5 polymorph isostructural with $I2/m$ indicated that such a structure is not competitive with $I4/m$ in terms of enthalpy.

The NF_6^- anion in $I4/m$ exhibits a slight tetragonal distortion at the low pressure limit (effectively 0 GPa) with two axial N–F bonds shorter by 1.3% than the four equatorial ones. Still all the bond lengths are very close to those obtained in molecular calculation (Table 1). The difference between the axial and equatorial bonds in $I4/m$ remains nearly constant with increasing pressure and does not exceed 1% at 300 GPa. Upon compression of $I4/m$ the N–F bonds in NF_4^+ shorten by 5% (to 1.25 Å at 300 GPa), while in case of the axial/equatorial bonds of NF_6^- the contraction is approximately 8%.

Above 151 GPa $I4/m$ is predicted to become thermodynamically less stable than a $P4/n$ structure ($Z=4$) containing a 1:1 ratio of NF_4^+ and NF_6^- , and no F^- anions. This polymorph is isostructural with the ambient pressure phase of $\text{PCl}_5 = (\text{PCl}_4^+)(\text{PCl}_6^-)^{41}$. In $P4/n$ the NF_6^- anions are more distorted compared to $I4/m$ with two unequal axial N–F bonds (Table 1 and Fig. 3). High pressure enhances this distortion with the difference between the two axial bonds reaching 10% at pressures above 20 GPa. This seems to indicate that in $P4/n$ the NF_6^- anion could be also described as a complex of square pyramidal NF_5 with an F^- anion (see Fig. 3). Unequivocal determination which of the two alternative descriptions (highly distorted NF_6^- vs $\text{NF}_5 \cdots \text{F}^-$ complex) is correct requires more elaborate calculations which are beyond the scope of this communication.

Interestingly there is no pressure region in which a structure containing NF_5 molecules would be the most stable polymorph of NF_5 . The $P-1$ structure, which contains such units, becomes more stable than $R3m/I-4$ at 78/243 GPa, but still in the whole pressure region studied it remains less stable than the NF_6^- -containing polymorphs ($I4/m$ and $P4/n$). The coordination of NF_5 molecules in the $P1$ phase changes from trigonal bipyramidal to square pyramidal above 40 GPa (Fig. 3). This transformation, which is in agreement with the predicted non-rigidity of the NF_5 molecule¹², is accompanied by a reduction in volume, and a change in the slope of the relative enthalpy (Fig. 2).

Discussion

The enthalpy change associated with the reaction: $\text{NF}_3 + \text{F}_2 \rightarrow \text{NF}_5$ becomes negative already at 40 GPa, as indicated by the grey region in Fig. 2. This shows that NF_5 , containing hypervalent nitrogen, could be synthesized from NF_3 and F_2 already at relatively low pressure, in the form of a novel salt $(\text{NF}_4^+)_2(\text{NF}_6^-)(\text{F}^-)$ ($I4/m$ polymorph). Furthermore, we found NF_5 to be stable against decomposition into NF_4 , another possible fluorine-rich phase of the N/F phase diagram (see Section III of the SI). Also, we emphasize that the calculated phonons remain positive within the whole Brillouin zone; a proof that the $I4/m$ phase is dynamically stable both at the pressure of synthesis (40 GPa) as well as at higher pressures (see section IV in SI).

Our results hint that the high-pressure oxidation of NF_3 by F_2 is accompanied by the ionization of the reactants, that is formation of NF_4^+ , NF_6^- and F^- ions in place of neutral NF_5 molecules. The tendency for heterolytic, rather than homolytic splitting of the F–F bond in F_2 reacting with NF_3 is further exemplified by the molecular-ionic transition observed in the $P1$ polymorph of NF_5 .

On a side note, we here point that for the related N/H system Qian *et al.* also predict formation of ionic species at high pressure and at large hydrogen contents²⁸. However these phases contain solely normal valent species

(NH_4^+ , H^+ , NH_2^- , H^-), in contrast to the hypervalent NF_5 , NF_6^- species reported in this study. Another difference is that for the N/H system the NH_5 composition is metastable with respect to decomposition into stable NH_3 and H_2 while we find NF_4 to be unstable at both ambient and high pressure. The instability of hypervalent N/H molecules can be traced back to the large steric crowding around the nitrogen atom in NH_n ($n > 4$) species. In fact, as calculated by Ewig and van Wazer, the NH_5 molecule is not only thermodynamically but also dynamically unstable in the gas phase, in contrast to NF_5 which is dynamically stable¹⁰.

The propensity for the formation of ionic phases at HP, observed also for other nitrogen compounds (NH_3 , N_2O)^{25,29,42}, can be explained by the pressure-induced increase of the lattice enthalpy (H_1) of ionic phases which leads to additional stabilization of such structures with respect to molecular, van der Waals bonded polymorphs. The increase in H_1 is a consequence of the volume reduction upon compression, as the lattice enthalpy is proportional to the inverse cube root of the molecular volume (the so-called Bartlett's relationship)^{43,44}.

Interestingly in the case of the NF_5 system the stabilization of ionic phases leads to larger than expected increase in hypervalency – the NF_6^- ion with a valence electron count of 12 is more stable at HP than the NF_5 containing 10 electrons in the nitrogen valence shell. We note that this is not a general trend; in the case of hypervalent XeF_2 the predicted pressure-induced ionization stabilizes a non-hypervalent salt of the $(\text{XeF}^+)(\text{F}^-)$ stoichiometry⁴⁵.

In summary our calculations indicate that a compound containing nitrogen(V) covalently bound by six fluorine atoms can be synthesized via a HP reaction between NF_3 and F_2 . A newly formed salt, of $(\text{NF}_4^+)_2(\text{NF}_6^-)(\text{F}^-)$ stoichiometry, would constitute the first example of a compound containing hypervalent nitrogen atoms. Most interestingly, due to relatively low pressures involved and due to the involvement of strong ionic interactions this new species might be stable even upon decompression to ambient pressure, particularly at low temperatures. Due to the computer-intensive nature of phonon calculations a detailed study of the dynamic stability of various NF_5 phases at low pressure is beyond the scope of this study.

Finally, it is also worth to remark that the phase transitions of NF_5 bear many similarities to those exhibited by PCl_5 , which serves as good example on the rule of thumb that at HP elements tend to resemble their heavier congeners¹⁵. We hope that the results presented here, which offer an intriguing extension of the palette of N/F binary compounds⁴⁶, will motivate experiments aimed at stabilizing the first genuine hexacoordinated binary compound of pentavalent nitrogen.

Methods

Hybrid potential calculations. Periodic DFT calculations utilized the HSE06 hybrid potential^{32–34}, while the PBE exchange correlation functional³⁵ was used in evolutionary searches, phonon calculations, and for comparative calculations. The projector augmented-wave (PAW) method was used, as implemented in the VASP 5.2 code^{47–49}. The cut-off energy of the plane waves was set to 1000 eV with a self-consistent-field convergence criterion of 10^{-6} eV. Valence electrons were treated explicitly, while standard VASP pseudopotentials were used for the description of core electrons. The k -point mesh was set at $2\pi \times 0.06 \text{ \AA}^{-1}$. All structures were optimized using a conjugate gradient algorithm until the forces acting on the atoms were smaller than 10 meV/Å. The abovementioned parameters ensured convergence of the calculated enthalpy within 2 meV per atom.

Structure searches. The candidate structures of NF_3 , F_2 , NF_5 , as well as NF_4 (see SI) were identified with the use of the USPEX evolutionary algorithm coupled with the PBE functional. Evolutionary searches were conducted for $Z = 1, 2, 3$, and 4 at $P = 50, 100, 200$ and 300 GPa. Due to the large computational cost of the HSE06 functional we were not able to employ it during the USPEX runs. Therefore, all of the best candidate structures obtained with USPEX were fully re-optimized (*i.e.* optimization of lattice parameters and internal coordinates) using the HSE06 functional. Beside the best structures identified at PBE level, we also used a number of enthalpically low lying meta-stable structures in the HSE06 re-optimization. For NF_3 our structure search identified the $Pnma$, $Pnma$ (2), and $P2_12_12_1$ molecular phases proposed in an earlier study⁵⁰, and did not find any new phases which would be competitive in terms of enthalpy with those three. The enthalpy change of the reaction $\text{NF}_{3(s)} + \text{F}_{2(s)} \rightarrow \text{NF}_{5(s)}$ was calculated taking (at each pressure) the lowest enthalpy polymorph of NF_5 and NF_3 , as well as the ambient-pressure α polymorph of F_2 ⁵¹. We note that above 50 GPa α - F_2 ($C2/c$ space group) symmetrizes spontaneously to a $Cmca$ structure which is analogous to the high-pressure polymorph of Cl_2 ⁵². Even at 300 GPa F_2 remains in the form of a molecular crystal.

Dispersion corrections. In order to determine the influence of dispersion-type interactions on the relative stability of NF_5 polymorphs we have calculated dispersion corrections (in the form of D3 correction proposed by Grimme and co-workers^{53–55}) for structures optimized at the HSE06 level of theory. We found that the D3 correction has very little to no influence on the relative stability of different NF_5 polymorphs (changes of transition pressures do not exceed 2 GPa upon inclusion of D3 corrections).

Structure visualization was performed with the VESTA 3.1 software⁵⁶. Symmetry recognition was performed with the online program FINDSYM⁵⁷.

References

- Christe, K. O., Guertin, J. P. & Pavlath, A. E. The tetrafluoronitronium(V) cation, NF_4^+ . *Inorg. Nucl. Chem. Lett.* **2**, 83–86 (1966).
- Miller, A. R., Tsukimura, R. R. & Velten, R. Fission-Fragment Synthesis of a New Nitrogen-Fluorine Compound. *Science* **155**, 688–688 (1967).
- Solomon, I. J., Keith, J. N. & Snelson, A. The decomposition of NF_4AsF_6 . *J. Fluor. Chem.* **2**, 129–136 (1972).
- Olah, G. A., Donovan, D. J., Shen, J. & Klopman, G. Onium ions. XVI. Hydrogen-deuterium exchange accompanying the cleavage of ammonium (tetra-deuterioammonium) trifluoroacetate by lithium deuteride (hydride) indicating SN2 like nucleophilic displacement at quaternary nitrogen through pentacoordinated ammonium hydride. *J. Am. Chem. Soc.* **97**, 3559–3561 (1975).
- Christe, K. O., Wilson, R. D. & Goldberg, I. B. Formation and decomposition mechanism of tetrafluoronitrogen (1+) salts. *Inorg. Chem.* **18**, 2572–2577 (1979).

6. Christe, K. O., Wilson, W. W., Schrobilgen, G. J., Chirakal, R. V. & Olah, G. A. On the existence of pentacoordinated nitrogen. *Inorg. Chem.* **27**, 789–790 (1988).
7. Rabenau, A. & Schulz, H. Re-evaluation of the lithium nitride structure. *J. Less Common Met.* **50**, 155–159 (1976).
8. Grohmann, A., Riede, J. & Schmidbaur, H. Electron-deficient bonding at pentacoordinate nitrogen. *Nature* **345**, 140–142 (1990).
9. Murrell, J. N. & Scollary, C. E. Non-empirical valence-shell self-consistent field molecular-orbital calculations on Group 5 tri- and penta-halides. *Dalton Trans.* 818–822 (1976).
10. Ewig, C. S. & Van Wazer, J. R. Ab initio studies of molecular structures and energetics. 3. Pentacoordinated nitrogen $\text{NF}_n\text{H}_{5-n}$ compounds. *J. Am. Chem. Soc.* **111**, 4172–4178 (1989).
11. Ewig, C. S. & Van Wazer, J. R. Ab initio studies of molecular structures and energetics. 4. Hexacoordinated NF_6^- and CF_6^{2-} anions. *J. Am. Chem. Soc.* **112**, 109–114 (1990).
12. Bettinger, H. F., Schleyer, P. V. R. & Schaefer, H. F. NF_5 Viable or Not? *J. Am. Chem. Soc.* **120**, 11439–11448 (1998).
13. Grant, D. J., Wang, T.-H., Vasiliu, M., Dixon, D. A. & Christe, K. O. F^+ and F^- affinities of simple N_xF_y and O_xF_y compounds. *Inorg. Chem.* **50**, 1914–1925 (2011).
14. Christe, K. O. & Wilson, W. W. Nitrogen pentafluoride: covalent NF_5 versus ionic NF_4^+F^- and studies on the instability of the latter. *J. Am. Chem. Soc.* **114**, 9934–9936 (1992).
15. Grochala, W., Hoffmann, R., Feng, J. & Ashcroft, N. W. The Chemical Imagination at Work in Very Tight Places. *Angew. Chem. Int. Ed. Engl.* **46**, 3620–3642 (2007).
16. Hemley, R. J. & Percy, W. Bridgman's second century. *High Press. Res.* **30**, 581–619 (2010).
17. Lee, R., Howard, J. A. K., Probert, M. R. & Steed, J. W. Structure of organic solids at low temperature and high pressure. *Chem. Soc. Rev.* **43**, 4300–4311 (2014).
18. Struzhkin, V. V. Superconductivity in compressed hydrogen-rich materials: Pressing on hydrogen. *Phys. C Supercond. its Appl.* **514**, 77–85 (2015).
19. Wang, H. *et al.* Nitrogen Backbone Oligomers. *Sci. Rep.* **5**, 13239 (2015).
20. Lu, C., Miao, M. & Ma, Y. Structural Evolution of Carbon Dioxide under High Pressure. *J. Am. Chem. Soc.* **135**, 14167–14171 (2013).
21. Miao, M. Caesium in high oxidation states and as a p-block element. *Nat. Chem.* **5**, 846–852 (2013).
22. Zhu, Q., Oganov, A. R. & Zeng, Q. Formation of Stoichiometric CsF_n Compounds. *Sci. Rep.* **5**, 7875 (2015).
23. Botana, J. *et al.* Mercury under Pressure acts as a Transition Metal: Calculated from First Principles. *Angew. Chem. Int. Ed. Engl.* **54**, 9280–9283 (2015).
24. Kurzydłowski, D. & Zaleski-Ejgierd, P. High-pressure stabilization of argon fluorides. *Phys. Chem. Chem. Phys.* **18**, 2309–2313 (2016).
25. Pickard, C. J. & Needs, R. J. Highly compressed ammonia forms an ionic crystal. *Nat. Mater.* **7**, 775–779 (2008).
26. Hu, A. & Zhang, F. A hydronitrogen solid: high pressure ab initio evolutionary structure searches. *J. Phys. Condens. Matter* **23**, 22203 (2011).
27. Yin, K., Wang, Y., Liu, H., Peng, F. & Zhang, L. N_2H : a novel polymeric hydronitrogen as a high energy density material. *J. Mater. Chem. A* **3**, 4188–4194 (2015).
28. Qian, G.-R. *et al.* Diverse Chemistry of Stable Hydronitrogens, and Implications for Planetary and Materials Sciences. *Sci. Rep.* **6**, 25947 (2016).
29. Palasyuk, T. *et al.* Ammonia as a case study for the spontaneous ionization of a simple hydrogen-bonded compound. *Nat. Commun.* **5**, 3460 (2014).
30. Ninet, S. *et al.* Experimental and theoretical evidence for an ionic crystal of ammonia at high pressure. *Phys. Rev. B* **89**, 174103 (2014).
31. Spaulding, D. K. *et al.* Pressure-induced chemistry in a nitrogen-hydrogen host-guest structure. *Nat. Commun.* **5**, 5739 (2014).
32. Heyd, J. & Scuseria, G. E. Efficient hybrid density functional calculations in solids: Assessment of the Heyd-Scuseria-Ernzerhof screened Coulomb hybrid functional. *J. Chem. Phys.* **121**, 1187–1192 (2004).
33. Krukau, A. V., Vydrov, O. A., Izmaylov, A. F. & Scuseria, G. E. Influence of the exchange screening parameter on the performance of screened hybrid functionals. *J. Chem. Phys.* **125**, 224106–1 (2006).
34. Heyd, J., Scuseria, G. E. & Ernzerhof, M. Hybrid functionals based on a screened Coulomb potential. *J. Chem. Phys.* **118**, 8207 (2003).
35. Perdew, J. P., Burke, K. & Ernzerhof, M. Generalized Gradient Approximation Made Simple. *Phys. Rev. Lett.* **77**, 3865–3868 (1996).
36. Glass, C. W., Oganov, A. R. & Hansen, N. USPEX—Evolutionary crystal structure prediction. *Comput. Phys. Commun.* **175**, 713–720 (2006).
37. Oganov, A. R. & Glass, C. W. Crystal structure prediction using ab initio evolutionary techniques: principles and applications. *J. Chem. Phys.* **124**, 244704 (2006).
38. Gillespie, R. J. & Nyholm, R. S. Inorganic stereochemistry *Q. Rev. Chem. Soc.* **11**, 339–380 (1957).
39. Boates, B. & Bonev, S. A. Electronic and structural properties of dense liquid and amorphous nitrogen. *Phys. Rev. B* **83**, 174114 (2011).
40. Finch, A., Fitch, A. N. & Gates, P. N. Crystal and molecular structure of a metastable modification of phosphorus pentachloride. *J. Chem. Soc. Chem. Commun.* 957–958 (1993).
41. Preiss, H. Strukturverfeinerung und Untersuchung der thermischen Schwingungen am festen Phosphor(V)-chlorid. *Z. Anorg. Allg. Chem.* **380**, 51–55 (1971).
42. Somayazulu, M. *et al.* Novel Broken Symmetry Phase from N_2O at High Pressures and High Temperatures. *Phys. Rev. Lett.* **87**, 135504 (2001).
43. Mallouk, T. E., Rosenthal, G. L., Mueller, G., Brusasco, R. & Bartlett, N. Fluoride ion affinities of germanium tetrafluoride and boron trifluoride from thermodynamic and structural data for $(\text{SF}_3)_2\text{GeF}_6$, ClO_2GeF_5 , and ClO_2BF_4 . *Inorg. Chem.* **23**, 3167–3173 (1984).
44. Jenkins, H. D. B., Roobottom, H. K., Passmore, J. & Glasser, L. Relationships among Ionic Lattice Energies, Molecular (Formula Unit) Volumes, and Thermochemical Radii. *Inorg. Chem.* **38**, 3609–3620 (1999).
45. Kurzydłowski, D., Zaleski-Ejgierd, P., Grochala, W. & Hoffmann, R. Freezing in resonance structures for better packing: XeF_2 becomes $(\text{XeF}^+)(\text{F}^-)$ at large compression. *Inorg. Chem.* **50**, 3832–3840 (2011).
46. Klapötke, T. M. Nitrogen–fluorine compounds. *J. Fluor. Chem.* **127**, 679–687 (2006).
47. Kresse, G. & Furthmüller, J. Efficiency of ab-initio total energy calculations for metals and semiconductors using a plane-wave basis set. *Comput. Mater. Sci.* **6**, 15–50 (1996).
48. Kresse, G. & Furthmüller, J. Efficient iterative schemes for ab initio total-energy calculations using a plane-wave basis set. *Phys. Rev. B* **54**, 11169–11186 (1996).
49. Kresse, G. & Joubert, D. From ultrasoft pseudopotentials to the projector augmented-wave method. *Phys. Rev. B* **59**, 1758–1775 (1999).
50. Kurzydłowski, D., Wang, H. B., Troyan, I. A. & Eremets, M. I. Lone-pair interactions and photodissociation of compressed nitrogen trifluoride. *J. Chem. Phys.* **141**, 64706 (2014).
51. Meyer, L., Barrett, C. S. & Greer, S. C. Crystal Structure of α -Fluorine. *J. Chem. Phys.* **49**, 1902–1907 (1968).
52. Johannsen, P. G. & Holzapfel, W. B. Effect of pressure on Raman spectra of solid chlorine. *J. Phys. C: Solid State Phys.* **16**, L1177–L1179 (2000).

53. Grimme, S., Antony, J., Ehrlich, S. & Krieg, H. A consistent and accurate ab initio parametrization of density functional dispersion correction (DFT-D) for the 94 elements H-Pu. *J. Chem. Phys.* **132**, 154104 (2010).
54. Grimme, S., Ehrlich, S. & Goerigk, L. Effect of the damping function in dispersion corrected density functional theory. *J. Comput. Chem.* **32**, 1456–1465 (2011).
55. Moellmann, J. & Grimme, S. DFT-D3 Study of Some Molecular Crystals. *J. Phys. Chem. C* **118**, 7615–7621 (2014).
56. Momma, K. & Izumi, F. VESTA : a three-dimensional visualization system for electronic and structural analysis. *J. Appl. Crystallogr.* **41**, 653–658 (2008).
57. Stokes, H. T. & Hatch, D. M. FINDSYM : program for identifying the space-group symmetry of a crystal. *J. Appl. Crystallogr.* **38**, 237–238 (2005).

Acknowledgements

D.K. and P.Z.-E. acknowledge the support from the Polish National Science Centre (NCN) within grants no. UMO-2014/13/D/ST5/02764, and UMO-2012/05/B/ST3/02467. This research was carried out with the support of the Interdisciplinary Centre for Mathematical and Computational Modelling (ICM) University of Warsaw under grant no GA65–26.

Author Contributions

D.K. conceived the idea of stabilizing NF_5 at high-pressure. D.K. and P.Z.-E. designed the research and carried out the calculations. Both authors analysed the results and wrote the manuscript.

Additional Information

Supplementary information accompanies this paper at <http://www.nature.com/srep>

Competing financial interests: The authors declare no competing financial interests.

How to cite this article: Kurzydłowski, D. and Zaleski-Ejgierd, P. Hexacoordinated nitrogen(V) stabilized by high pressure. *Sci. Rep.* **6**, 36049; doi: 10.1038/srep36049 (2016).

Publisher's note: Springer Nature remains neutral with regard to jurisdictional claims in published maps and institutional affiliations.



This work is licensed under a Creative Commons Attribution 4.0 International License. The images or other third party material in this article are included in the article's Creative Commons license, unless indicated otherwise in the credit line; if the material is not included under the Creative Commons license, users will need to obtain permission from the license holder to reproduce the material. To view a copy of this license, visit <http://creativecommons.org/licenses/by/4.0/>

© The Author(s) 2016